Korea-Australia Rheology Journal
Vol. 14, No. 2, June 2002 pp. 77-86

A microscopic study on the rheological properties of human blood in low concentration limit

In Seok Kang*
Department of Chemical Engineering and Division of Mechanical and Industrial Engineering, Pohang University of Science and Technology, San 31 Hyoja-dong, Nam-gu, Pohang 790-784, Korea
(Received: May 7, 2002)

Abstract

A microscopic theoretical study is performed to predict the rheological properties of human blood in the low concentration limit. The shear thinning behavior of blood in the low shear limit is studied by considering the aggregate formation of red blood cells, which is called the rouleaux formation. Then the constitutive equations of blood in the high shear limit are derived for various flow situations by considering the unique features of deformation of blood cells. Specifically, the effects of the surface-area-preserving constraint and the tank-treading motion of blood cells on the rheological properties are studied.

1. Introduction

In the present paper, we are concerned with development of a theory on the rheological properties of human blood by viewing the blood as a suspension of red blood cells (RBCs). More specifically, we want to derive formulas for the effective viscosity of blood in various basic flow fields by taking account of the behavior of red blood cells such as aggregation in the low shear rate limit and the area-preserving deformation in the high shear rate limit.

The experimental findings from the viscosity measurements indicate the so-called shear thinning behavior of blood. Thus, in many numerical studies, the empirical constitutive relations such as Casson's model and the biviscosity model are adopted (see the book by Fung (1981) and the paper by Nakamura & Sawada (1988)).

However, the viscometric measurement results are not sufficient, because it can provide only the rheological information of the blood under certain limited flow fields such as a capillary flow or a shear flow. On the other hand, in real situations, the blood is to be subjected to much more diverse flow fields. Therefore, it is necessary to perform theoretical studies on the rheological properties along with the viscometric measurements. In such theoretical studies, the blood is viewed as a suspension of red blood cells. The microscopic information of the behavior of blood cells is incorporated with the theory of suspension rheology to derive the macroscopic rheological properties.

As a first attempt in that direction, the shear thinning behavior of blood in the low shear limit is studied from a microscopic point of view. Then, the constitutive equations of blood in the high shear rate limit are also derived by considering the deformation characteristics of the blood cells.

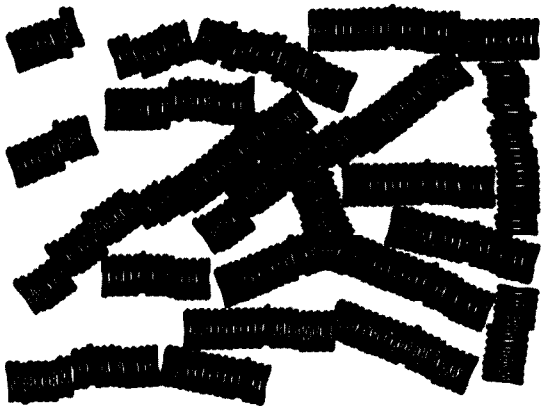

Fig. 1. Rouleaux of human red blood cells.

2. Behavior of red blood cells

When the shear rate is small, the red blood cells form rouleaux by aggregation as shown in Fig. 1 (see also Fung 1981). As the shear rate increases, the average number of red blood cells in each rouleau decreases. If the shear rate is larger than a certain critical value, the rouleau is broken up into individual cells. At subcritical shear rates, the red blood cells in each rouleau maintain their rest-state equilibrium shape, i.e. doughnut-like shape. However, if the shear rate is supercritical, the red blood cells are dispersed in plasma separately and exhibit quite complicated behav-

*Corresponding author: iskang@postech.ac.kr

ior of deformation and motion.

Schmidt-Schönbein *et al.* (1969) found the following from *in vitro* experiments on the blood at low concentration of RBC (5-10%). Normal cells were observed to be separate, not in rouleaux, at shear rate κ=4.6 s^{-1}. Upon slight increase of κ the individual cells were seen with occasional tumbling and orbiting in flow. As κ was further increased the cells became oriented and less orbiting was seen. For κ>100 s^{-1} the individual cells lost their biconcave shape and transformed to a variety of shapes, many resembling prolate ellipsoids with major axes parallel to the direction of flow, with no tumbling. Goldsmith (1971) reported similar observation from the Poiseuille flow experiment. In summary, the experimental evidence suggests that at low shear rates the cells rotate but as the flow speeds up rotation is no longer observed, i.e. the profile of the cell becomes stationary relative to axes fixed in space. This kind of motion is called the tank-treading motion (see the schematic figure given later in subsection 5.2). Theoretical studies for this tank-treading motion were made by Richardson (1974) and Keller and Skalak (1982).

Another important feature we must consider is the so-called constraint of area preservation during the deformation of blood cells. This constraint and the flexibility of cell membrane constitute a unique feature of blood cell deformation. Due to the constraint of area preservation and negligible resistance to bending, the equilibrium shape of red blood cells does not depend on the strain rate if its value is larger than a certain critical value. Instead, the membrane tension increases as the strain rate increases, and eventually the cell is broken apart (i.e. hemolysis occurs) if the strain rate is larger than a critical value. Pozrikidis (1990) showed that a spheroidal shape, which is determined by the sphericity index rather than the strain rate, is an equilibrium shape of a blood cell subjected to a uniaxial straining flow.

In the present study, the above characteristics of blood cells are considered to predict the effective viscosity of blood as a function of shear rate. For our theoretical development, Batchelor's theory on the suspension of ellipsoidal particles is used.

3. Theories on the suspension rheology

3.1. Batchelor's theory

Batchelor (1970) used the volume average to derive the formula for the bulk stress from a microscopic flow information.

$$\Sigma_{ij} = \frac{1}{V}\int(\sigma_{ij}-\rho u_i' u_j')dV \tag{3.1}$$

With the aid of vector calculus, he showed that

$$\Sigma_{ij} = -\delta_{ij} \int_{V-\sum V_0} pdV+\mu\left(\frac{\partial U_i}{\partial x_j}+\frac{\partial U_j}{\partial x_i}\right)+\Sigma_{ij}^{(p)} \tag{3.2}$$

where V_0 denotes the volume of each particle and

$$\Sigma_{ij}^{(p)} = \frac{1}{V}\sum\int_{A_0}\{\sigma_{ik}x_j n_k-\mu(u_i n_j+u_j n_i)\}dA$$

$$-\frac{1}{V}\sum\int_{V_0}\rho f_i' x_j dV-\frac{1}{V}\int\rho u_i' u_j' dV \tag{3.3}$$

The term $\Sigma_{ij}^{(p)}$ is called the 'particle stress', and $\frac{\partial U_i}{\partial x_j}$ is the average velocity gradient. In fact, (3.2) is a quite general expression and may be a starting point for the suspension rheology for various situations.

Batchelor applied the formula (3.2) to the case of dilute suspension ($\phi\rightarrow 0$) to get some analytical results. He assumed further that the particle Reynolds number is very small and the last two terms in (3.3) may be safely neglected. In the case of dilute suspension, the interaction between particles is neglected and consideration of a single particle in a general linear flow provides sufficient information. Thus, the average velocity gradient equals the velocity gradient given far from the particle.

$$\partial U_i/\partial x_j = e_{ij}-\varepsilon_{ijk}\Omega_k \tag{3.4}$$

Batchelor showed that the particle stress in the dilute limit can be represented by

$$\Sigma_{ij}^{(p)} = \frac{4\pi\mu}{V}\sum D_{ij} \tag{3.5}$$

where D_{ij} is the coefficient in the expansion for the disturbance pressure and the disturbance vorticity

$$\frac{p'}{\mu} = -D_j\frac{\partial r^{-1}}{\partial x_j}-D_{jk}\frac{\partial^2 r^{-1}}{\partial x_j\partial x_k}+\cdots, \tag{3.6}$$

$$\omega_i' = -\varepsilon_{ijk}D_j\frac{\partial r^{-1}}{\partial x_k}-\varepsilon_{ijk}D_{jl}\frac{\partial^2 r^{-1}}{\partial x_k\partial x_l}+\cdots. \tag{3.7}$$

The effective stress of a dilute suspension of ellipsoidal particles has in general non-Newtonian form and shows complicated behavior. However, in some special situations, the constitutive equation can be derived without much difficulty. The first example is the suspension of couple-free particles which are similar in shape and orientation. For this case, Batchelor showed that

$$\Sigma_{ij}^{(p)} = 3\mu e_{kl}\frac{C_{ijkl}}{abc}\frac{\sum\frac{4}{3}\pi abc}{V} \tag{3.8}$$

for the suspension of ellipsoidal particles with semi-diameters a, b, and c. Another example is the case of couple-free particles subject to such strong Brownian motion that their orientations are randomly distributed with uniform probability, i.e. statistically isotropic case. In this case,

$$\Sigma_{ij}^{(p)} = 2\mu e_{ij}\frac{4\pi}{3V}\sum abc\left\{\frac{4(J_1+J_2+J_3)}{15(J_1J_2+J_2J_3+J_3J_1)}+\frac{2}{5}\left(\frac{1}{I_1}+\frac{1}{I_2}+\frac{1}{I_3}\right)\right\}. \tag{3.9}$$

where I_i and J_i (i = 1 , 2, 3) are the functions of a, b, and c. The above two expressions are used to predict the effective viscosity of the blood.

3.2. Hinch and Leal's theory

Hinch and Leal (1971) applied Batchelor's general formulation to the suspension rheology of dilute spheroidal particles. Their principal result is

$$\Sigma^{(p)} = 2\mu\phi\{2A_H\boldsymbol{E}:\langle\boldsymbol{pppp}\rangle + 2B_H\left(\boldsymbol{E}\cdot\langle\boldsymbol{pp}\rangle+\langle\boldsymbol{pp}\rangle\cdot\boldsymbol{E}-\frac{2}{3}\boldsymbol{IE}:\langle\boldsymbol{pp}\rangle\right) + C_H\boldsymbol{E}+F_HD_r+\left(\langle\boldsymbol{pp}\rangle-\frac{1}{3}\boldsymbol{I}\right)\} \tag{3.10}$$

where $\boldsymbol{E}$ is the rate-of-strain tensor ($\boldsymbol{E} = e_{ij}\,\boldsymbol{e}_i\,\boldsymbol{e}_j$), $\boldsymbol{p}$ is the unit vector in the direction of rotation axis, and D_r is the rotary diffusivity. By using Batchelor's general result for the ellipsoidal particles, they derived the asymptotic formulas for the coefficients when the particles are spheroidal.

4. Effect of aggregation on the effective properties of blood in the low shear rate limit

The human blood cells are known to form aggregates that are called rouleaux. When the shear rate is small, the aggregates become prevalent. In this section, we explore the effect of aggregation on the effective properties of human blood. As a first attempt, we assume that the degree of aggregation is the same for all rouleaux and each roubleau can be approximated by a spheroid as shown in Fig. 2. We shall consider two extreme cases of orientation distribution: one is the random distribution, which may be appropriate for low shear rate limit; and the other is the completely aligned situation in the uniaxial straining flow.

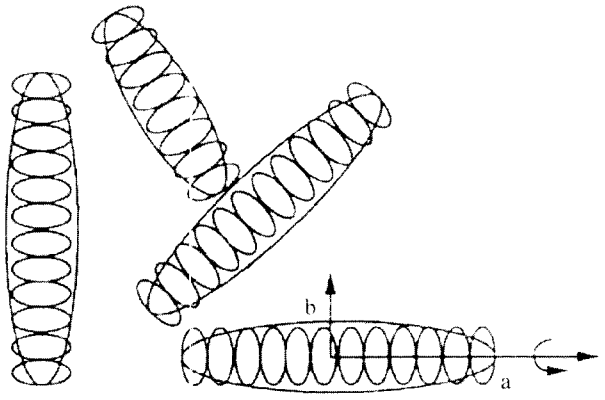

Fig. 2. The spheroidal approximation for the rouleaux formed by aggregation at low shear rates.

4.1. Randomly oriented spheroidal rouleaux

Let us begin with the case of the perfect random distribution of orientation. When the suspension is dilute, Batchelor's formula (3.9) is appropriate for the particle stress term. The formula can be further simplified when the shape of the particle is spheroidal (i.e., $b = c$)

$$\Sigma_{ij}^{(p)} = 2\mu e_{ij}\phi\left\{\frac{4(J_1+2J_2)}{15(2J_1+J_2)J_2}+\frac{2}{5}\left(\frac{1}{I_1}+\frac{2}{I_2}\right)\right\}, \tag{4.1}$$

where ϕ is the volume fraction of solid particles. Since ab^2=1 for spheroids, the formula (4.1) can be represented as (see Kang (1993) for the details)

$$\Sigma_{ij}^{(p)} = 2\mu e_{ij}\phi f(a), \tag{4.2}$$

where a is the dimensionless semi-diameter of the rouleau along the rotation axis. Therefore, the effective viscosity of blood is given by

$$\mu^* = \mu(1 + f(a)\phi). \tag{4.3}$$

where μ is the viscosity of plasma.

When the rouleaux are quite long, we may express the dimensionless semi-diameter a in terms of degree of aggregation. Let n be the number of cells in one rouleau. Since the maximum thickness of a cell is about 2.8 μm and the diameter is 7.6 μm, a n-cell rouleau has the aspect ratio about

$$r = \frac{a}{b} = a^{\frac{3}{2}} = \frac{2.8}{7.6}n$$

and thus

$$a = \frac{n^{\frac{2}{3}}}{2}. \tag{4.4}$$

In Fig. 3, the factor $(f(a) = f(n^{\frac{3}{2}}/2) = \tilde{f}(n))$ is shown as a function of the degree of aggregation. In order to see the effect of aggregation more explicitly, we may consider

$$\frac{\mu^*(n)}{\mu^*(1)} = \frac{1+\tilde{f}(n)\phi}{1+\tilde{f}(1)\phi} \tag{4.5}$$

where $\mu^*(n)$ denotes the effective viscosity when the degree of aggregation is n. Even though the above result was derived for the low concentration limit, let us apply it to the case of normal hematocrit ϕ=0.45. Then, with $\tilde{f}(1) = 2.8$, $\tilde{f}(20) = 4.3$, $\tilde{f}(40) = 8.7$, $\tilde{f}(80) = 22.5$, we have

$$\frac{\mu^*(n)}{\mu^*(1)} = \begin{cases} 1.3, & \text{for } n = 20 \\ 2.2, & \text{for } n = 40 \\ 4.9, & \text{for } n = 80 \end{cases}. \tag{4.6}$$

As we can see above, the effect of aggregation is considerable even when the low concentration model is used. In fact, if the concentration is as high as ϕ=0.45, we need to consider the interaction effects between the rouleaux. Although extremely complicated physics of interaction

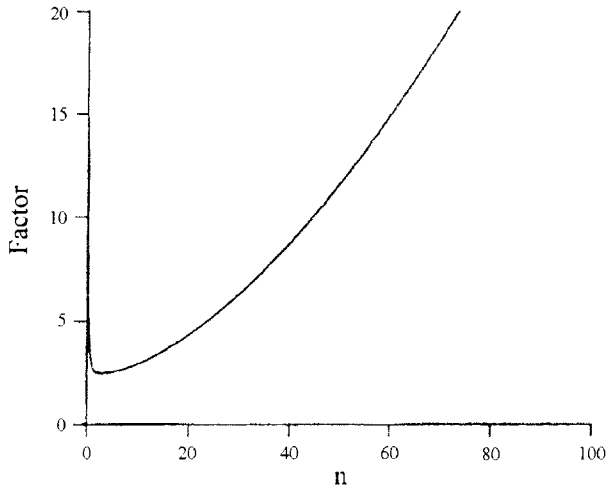

Fig. 3. The factor function $\tilde{f}(n)$ for the effective viscosity as given in (4.5).

does not allow us any rigorous analysis, an order of increase in the effective viscosity can be easily imagined as observed in experiments (e.g. Chien, 1970).

The significance of the present analysis lies in that the shear thinning behavior of blood at low shear rates can be best understood by the fact that the degree of aggregation decreases as the shear rate increases.

4.2. Aligned spheroidal rouleaux in the uniaxial straining flow

When the rouleaux are subjected to the straining flow, they are aligned in the principal strain direction as shown in Fig. 4. In this case, the effective viscosity may be easily obtained. The rate-of-strain tensor for this problem is

$$e_{ij} = E\left[p_i p_j - \frac{1}{2}q_i q_j - \frac{1}{2}r_i r_j\right] \tag{4.7}$$

For spheroidal particles, we may show that (Batchelor, 1970)

$$\frac{C_{ijkl}e_{kl}}{abc} = E\frac{J_1\left(p_i p_j - \frac{1}{3}\delta_{ij}\right) - \frac{J_2}{2}\left(q_i q_j + r_i r_j - \frac{2}{3}\delta_{ij}\right)}{\frac{3}{4}(2J_1 + J_2)J_2} = \frac{4}{9J_2}e_{ij} \tag{4.8}$$

Then from (3.8), we have

$$\Sigma_{ij}^{(p)} = 2\mu e_{ij}\phi\left(\frac{2}{3J_2}\right) \tag{4.9}$$

Therefore, the effective viscosity is given by

$$\mu^* = \mu[1 + f(a)\phi] = \mu\left[1 + \left(\frac{2}{3J_2}\right)\phi\right] \tag{4.10}$$

The factor for the uniaxial straining flow case (2/3 J_2) is shown in Fig. 5 for comparison with the factor for the case of complete random distribution.

4.3. Breakup of rouleaux due to straining flows

In order to proceed in the development of the theory for the shear thinning effect, we need to estimate the degree of aggregation in terms of shear rate. As a first step, we consider a rouleau subject to a uniaxial straining flow as shown in Fig. 4. Although the rouleaux are known to be deformed easily in shear flows, the major cause of rouleau breakup is believed to be the straining component of the imposed shear flow. Thus, by considering only the uniaxial straining flow we may achieve the goal. The straining force exerted on the center-plane of a rouleau can be estimated. If the straining force is larger than the attracting force between cells in a rouleau, then the rouleau is broken up into two smaller rouleaux.

As before, we again approximate a rouleau as a spheroid as shown in Fig. 4. Then the straining force can be easily

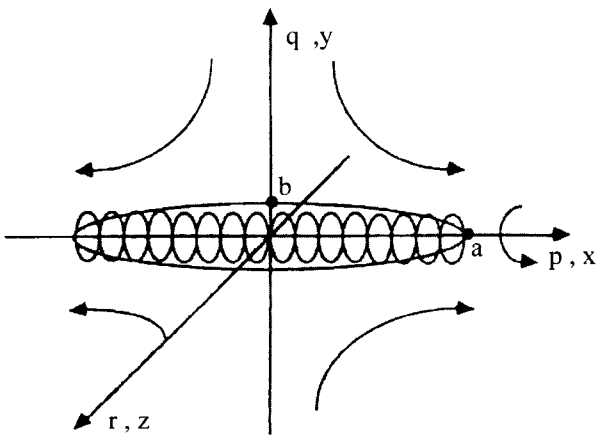

Fig. 4. A completely aligned rouleau in a uniaxial straining flow.

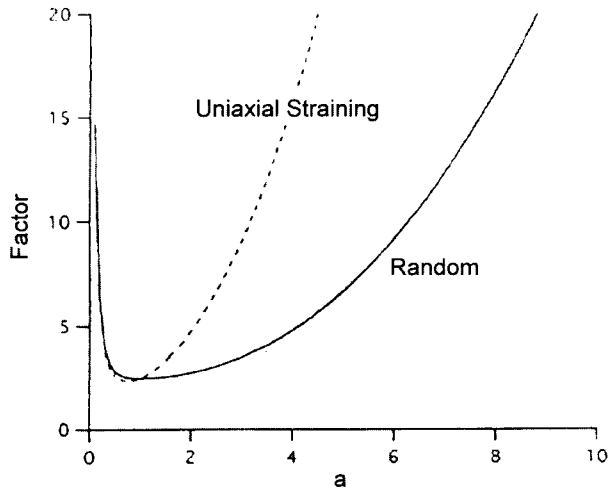

Fig. 5. The factor functions of the effective viscosities for the aligned rouleaux in a uniaxial straining flow and the randomly distributed rouleaux.

obtained by Jeffery's solution (1922). As discussed in Pozrikidis (1990), the surface stress acting on the external surface of an ellipsoidal particle, which is immersed in a general linear flow, is given by

$$\boldsymbol{f}_1 = (-P_0\boldsymbol{I}+\boldsymbol{A})\cdot\hat{\boldsymbol{n}},$$

where $\hat{\boldsymbol{n}}$ is the outward unit normal from the surface of the particle. The constant matrix A is diagonal if a uniaxial straining flow is assumed and the x-directional component of the surface stress is given in dimensionless form as

$$f_x = (A_{11}-P_0)\hat{\boldsymbol{n}}\cdot\boldsymbol{e}_x \tag{4.11}$$

Since the stress is scaled by $\mu E/2$ for the rate-of-strain tensor

$$\boldsymbol{E} = E\left[\boldsymbol{e}_x\boldsymbol{e}_x-\frac{1}{2}\boldsymbol{e}_y\boldsymbol{e}_y-\frac{1}{2}\boldsymbol{e}_z\boldsymbol{e}_z\right] \tag{4.12}$$

the straining force on the right half of the rouleau is easily obtained by integrating the surface stress

$$\tilde{F}_x = \int\tilde{f}_x dS = \left[A_{11}\left(\frac{\mu E}{2}\right)-p_0\right]\int(\hat{\boldsymbol{n}}\cdot\boldsymbol{e}_x)dS = \left[A_{11}\left(\frac{\mu E}{2}\right)-p_0\right](\pi b^2) \tag{4.13}$$

Now let the dimensional maximum attracting force per unit area of cell-cell interface be $\tilde{f}_{att}$. Then

$$\tilde{F}_{att} = \tilde{f}_{att}(\pi b^2) \tag{4.14}$$

In order for a rouleau to be broken up by straining flow $\tilde{F}_x \geq \tilde{F}_{att}$. Therefore at critical aggregation, we have

$$A_{11}\left(\frac{\mu E}{2}\right) = p_0+\tilde{f}_{att} \tag{4.15}$$

As given in Pozrikidis (1990), $A_{11} = \frac{8}{3g_2''}$. The function $g_2''(r)$ can be shown to be identical to the function $J_2(a)$ of Batchelor's notation by using the relation $r=a/b=a^{3/2}$

$$g_2''(r) = \int_0^\infty \frac{udu}{\left(E^{\frac{4}{3}}+u\right)^{\frac{3}{2}}\left(E^{-\frac{2}{3}}+u\right)^2} = \int_0^\infty \frac{\lambda d\lambda}{(a^2+\lambda)^{\frac{3}{2}}\left(\frac{1}{a}+\lambda\right)^2} = J_2(a) \tag{4.16}$$

Now we have the relationship

$$\left(\frac{4}{3J_2}\right)(\mu E) = p_0+\tilde{f}_{att}. \tag{4.17}$$

Let us now estimate the attracting force. Chien (1970) showed experimentally that the rouleau may be formed if the shear rate is less than 4 $\sec^{-1}$. Let the maximum value of the strain rate be E_{max}, beyond which the rouleau formation is not observed. Then for 2-*cell* rouleau we may apply (4.17) to estimate E_{max}. For convenience, we adopt a reasonable approximation that a 2-*cell* rouleau may be viewed as a sphere. For this case, we can show that (Batchelor, 1970)

$$\frac{2}{3J_2} = \frac{5}{2}.$$

Therefore, we have

$$p_0+\tilde{f}_{att} = 5\mu E_{max}. \tag{4.18}$$

Finally from (4.17) and (4.18), we find a very important relationship

$$\frac{E}{E_{max}} = \frac{15}{4}J_2(a), \tag{4.19}$$

which is one of the most important results in the present work. The definition of $J_2(a)$ for the axisymmetric case is given in (4.16).

Now the relation (4.19) can be used to get a formula for the effective viscosity that exhibits shear thinning behavior. As discussed in subsection 4.1, the effective viscosity may be found if we have the degree of aggregation \$n\$ by the formula (4.3) via (4.4). Thus, we have

$$\frac{\mu^*(n)}{\mu^*(sph)} = \frac{1+\tilde{f}(n)\phi}{1+\tilde{f}(sph)\phi} \tag{4.20}$$

where $\mu^*(sph)$ denotes the effective viscosity of the suspension of spherical particles. On the other hand, from (4.19), we may estimate the the dimensionless semi-diameter, a, of a rouleau for the given dimensionless strain rate E/E_{max}. In turn, the degree of aggregation n can be found by the relation (4.4) for the given value of a. In that way, the degree of aggregation n can be estimated as a function of the dimensionless strain rate E/E_{max}.

Since now the degree of aggregation is known for the given dimensionless strain rate, the effective viscosity can be computed by using the relation (4.20). In Fig. 6, the effective viscosity is given as a function of dimensionless strain rate for the case of hematocrit ϕ=0.45. The shear thinning effect is clearly seen and the result shows qualitatively good agreement with the experimental findings of Chien (1970). Of course, our analysis is based on the theory for the dilute suspension. Furthermore, we did not include any complicated aggregation behavior such as the branched rouleau formation and the deformation of a rouleau in shear flows. Nevertheless, the simple theory demonstrates clearly that the aggregation of blood cells accounts for the interesting shear thinning behavior of human blood at low shear rates.

5. Effect of area preserving constraint on the effective properties in the high shear rate

In the previous section, we have developed a theory that predicts the shear thinning behavior based on the rouleau formation in the low shear rate limit. In this section, we consider now the case of high shear rate. When the shear rate is high enough for the cells to exist separately in plasma, the effective property of blood is determined mainly by the deformation

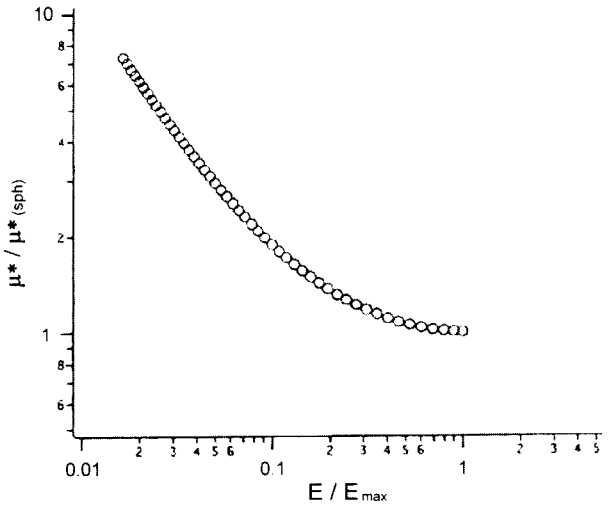

Fig. 6. The dimensionless effective viscosity as a function of dimensionless strain rate.

and motion of individual cells. In this section, we consider the following: (i) the effects of completely aligned cells in axisymmetric straining flows; and (ii) the effect of tank-treading motion of red blood cells due to shear flow.

5.1. Completely aligned cells in axisymmetric straining flows

We first consider the simplest case, in which individual cells are completely aligned due to the axisymmetric straining flows. As discussed in section 2, the red blood cells are easily deformed in straining flows and take spheroidal equilibrium shapes in axisymmetric straining flows if the membrane tension is assumed to be isotropic. Since the cell deformation should satisfy the simultaneous requirements of volume conservation and the area preserving, the nature of cell deformation is different from that of elastic particles or droplets. Differently from the case of elastic particles, the equilibrium shape is independent of the strain rate if the bending resistance of the cell is neglected. On the other hand, the tension of the membrane increases as the strain rate increases. In this section, the effect of area-preserving property on the suspension rheology is discussed for the two axisymmetric straining flows. In a uniaxial straining flow each blood cell is deformed into prolate shape and in a biaxial straining flow into oblate shape as shown in Fig. 7.

The most important parameter for the deformation of blood cells is the sphericity index S defined by

$$S = \frac{(A/4\pi)^{\frac{1}{2}}}{(3V/4\pi)^{\frac{1}{3}}}$$

where A is the total surface area and V is the volume of the cell. For the case of spheroidal particles, the index is a function

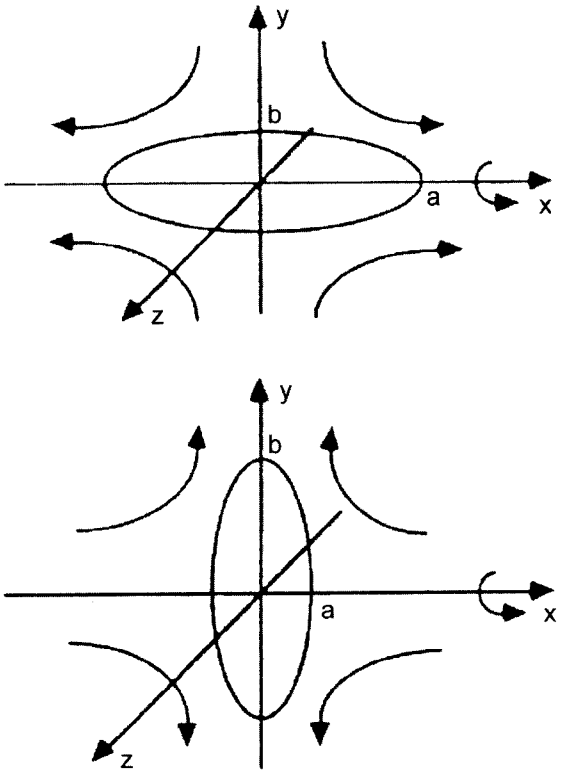

Fig. 7. The prolate and oblate blood cells in the uniaxial and biaxial straining flows.

of the the aspect ratio $r=a/b$. For the sphericity index of the human red blood cell, it is well established that the area of a red cell is approximately 44% larger than the minimum area required for the spherical shape (Skalak *et al.*, 1989). Then by the definition of the index we have S=1.2 and we have

$$r = 0.25 \quad \text{for an oblate spheroid} \tag{5.1a}$$

$$r = 6 \quad \text{for an prolate spheroid} \tag{5.1b}$$

Now let us first discuss the case of uniaxial straining flow, in which the red blood cell takes a prolate equilibrium shape. As in section 4, the effective viscosity can be obtained by using the theory of Batchelor or equivalently by using the theory of Hinch and Leal. Here let us use the theory of Hinch and Leal (1971) that is given in subsection 3.2. When the aspect ratio r=6, the coefficients in (3.10) can be estimated as (see Hinch and Leal, 1971)

A_H=9.1379, B_H=0.05430, C_H=2.

When the effect of Brownian motion is neglected, from (3.10), we have

$$\Sigma^{(p)} = 2\mu\phi\{18.2758\boldsymbol{E}:\langle pppp\rangle$$

$$+0.1086\left(\boldsymbol{E}\cdot\langle pp\rangle+\langle pp\rangle\cdot\boldsymbol{E}-\frac{2}{3}\boldsymbol{I}\boldsymbol{E}:\langle pp\rangle\right)+2\boldsymbol{E}\} \tag{5.2}$$

In the case of uniaxial straining flow, all cells are assumed to be oriented in the e_x-direction and thus

$$\boldsymbol{p} = \boldsymbol{e}_x\,;\quad \boldsymbol{E} = E\left[\boldsymbol{e}_x\boldsymbol{e}_x - \frac{1}{2}\boldsymbol{e}_y\boldsymbol{e}_y - \frac{1}{2}\boldsymbol{e}_z\boldsymbol{e}_z\right],$$

where E is the principal strain rate. Substituting the above relations into (5.2) and subtracting the isotropic contribution, we find

$$\Sigma^{(p)} = 2\mu\phi(14.3287)\boldsymbol{E}\,. \tag{5.3}$$

Or we have

$$\mu^* = \mu(1 + 14.33\phi) \tag{5.4}$$

In the case of biaxial straining flow, the aspect ratio of the equilibrium cell shape is $r = 0.25$ and the coefficients are estimated as

$$A_H = 2.2929,\ B_H = -1.91815,\ C_H = 4.8363.$$

By substituting the above coefficients, $\boldsymbol{p} = \boldsymbol{e}_x$ and

$$\boldsymbol{E} = E\left[-\boldsymbol{e}_x\boldsymbol{e}_x + \frac{1}{2}\boldsymbol{e}_y\boldsymbol{e}_y + \frac{1}{2}\boldsymbol{e}_z\boldsymbol{e}_z\right],$$

and subtracting the isotropic contribution, we find

$$\Sigma^{(p)} = 2\mu\phi(2.7784)\boldsymbol{E}\,. \tag{5.5}$$

Therefore, the effective viscosity for the biaxial straining flow is

$$\mu^* = \mu(1 + 2.78\phi). \tag{5.6}$$

The effective viscosity for a dilute suspension of elastic particles was obtained by Cho (1992) under the assumption that the deformation from spherical shape is not large. The result is that

$$\Sigma^{(p)} = 2\mu\phi\left[\frac{5}{2} \pm 2.6786\delta + 15.386\delta^2\right]\boldsymbol{E};\quad \delta = \frac{\mu E}{G}, \tag{5.7}$$

where $\pm$ refers to the uniaxial and biaxial straining flows respectively, and E and G are the principal strain rate and the shear modulus of the elastic particle. The effective viscosity corresponding to (5.7) is

$$\mu^* = \mu\left[1 + \left(\frac{5}{2} \pm 2.6786\delta + 15.386\delta^2\right)\phi\right];\quad \delta = \frac{\mu E}{G}. \tag{5.8}$$

The factors for the effective viscosity $(\mu^*-\mu)/\phi$ are shown in Fig. 8. The closed and open circles are for the effective viscosity of human blood in the cases of uniaxial and biaxial straining flows respectively. The open and closed triangles are for the effective viscosity of the suspension of elastic particles in the cases of uniaxial and biaxial straining flows. For the cases of elastic particles, μ/G=0.01s is used in the plot.

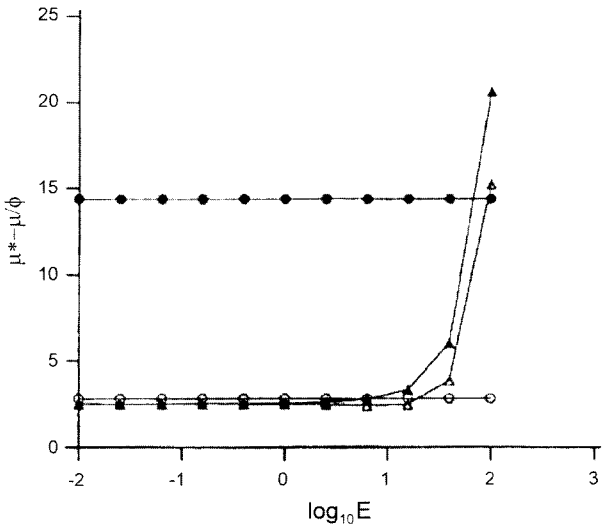

Fig. 8. The factors of the effective viscosity $(\mu^*-\mu)/\phi$ as functions of strain rate (closed circles: RBC in a uniaxial straining flow; open circles: RBC in a biaxial straining flow; closed triangles: elastic particle in a uniaxial straining flow; open triangles: elastic particle in a biaxial straining flow).

5.2. The effect of tank-treading motion in shear flow

Here we estimate the bulk stress of human blood subject to shear flow by considering the tank-treading motion of red blood cells as shown in Fig. 9. In order to develop a theory on the effective viscosity, Batchelor's (1970) theory for the dilute suspension of ellipsoidal solid particles is modified appropriately to consider the tank-treading motion of red blood cells. Then the modified theory is incorporated with the theory of Keller and Skalak (1982) on the tank-treading motion of red cells to estimate the rheological properties of blood.

5.2.1. Disturbance field near a tank-treading red blood

As we have seen in 3.1, we need to obtain the second order tensor D_{ij} for estimation of $\Sigma_{ij}^{(p)}$. To do that, we consider a tank-treading ellipsoidal red blood cell as shown in Fig. 9. In the figure, x_i denote the coordinates in a fixed Cartesian coordinate system and $\bar{x}_i$ denote coordinates in a second Cartesian system having origin coinciding with the fixed frame. The x_3 axis is assumed to coincide with $\bar{x}_3$ axis, but $\bar{x}_1$ and $\bar{x}_2$ axes are rotated through an angle θ with respect to the x_1 and x_2 axes. The ellipsoidal surface is defined by the semi-axes a, b, and c on $\bar{x}_1$, $\bar{x}_2$, and $\bar{x}_3$, respectively. The membrane surface velocity v_i^m relative to and referred to the body frame is assumed to be

$$\bar{v}_1^m = v(-a/b)\bar{x}_2,\quad \bar{v}_2^m = v(b/a)\bar{x}_1,\quad \bar{v}_3^m = 0 \tag{5.9}$$

where v is a parameter having the dimension of frequency.

For an ellipsoidal particle with the surface velocity in the

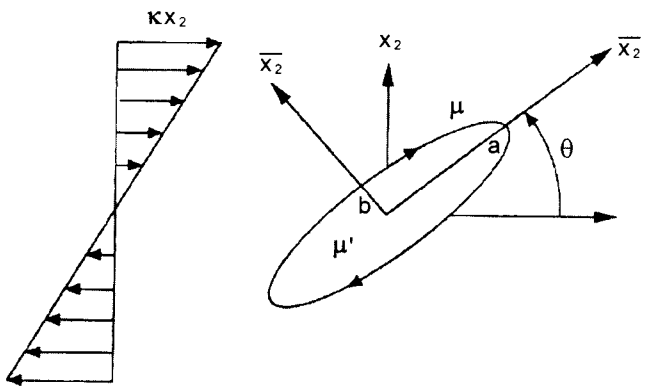

Fig. 9. An ellipsoidal red blood cell undergoing tank-treading motion due to a shear flow.

form

$$\bar{v}_i^m = (\bar{E}_{ij}^m + \bar{\Omega}_{ij}^m)\bar{x}_j \tag{5.10}$$

in the flow field which has

$$\bar{U}_i = (\bar{E}_{ij} + \bar{\Omega}_{ij})\bar{x}_j \tag{5.11}$$

far from the particle, Roscoe (1967) showed that the disturbance is the same as would be produced by a rigid, non-rotating ellipsoid in a liquid undergoing the undisturbed flow

$$\bar{U}_i^0 = (\bar{E}_{ij} - \bar{E}_{ij}^m)\bar{x}_j + (\bar{\Omega}_{ij} - \bar{\Omega}_{ij}^m)\bar{x}_j, \tag{5.12}$$

where the barred quantities are referred to the moving coordinate system.

The disturbance flow field is generated by the rate-of-strain tensor $(E_{kl} - E_{kl}^m)$, which are the components of the tensor $\boldsymbol{E}$ - $\boldsymbol{E}^m$ referred to the fixed frame. Hence we have

$$D_{ij} = C_{ijkl}(E_{kl} - E_{kl}^m) \tag{5.13}$$

For the shear flow,

$$E_{ij} = \frac{\kappa}{2}\begin{pmatrix} 0 & 1 & 0 \\ 1 & 0 & 0 \\ 0 & 0 & 0 \end{pmatrix}. \tag{5.14}$$

From the surface membrane velocity, we have

$$\bar{E}_{ij}^m = \left(\frac{a^2-b^2}{2ab}\right)\begin{pmatrix} 0 & 1 & 0 \\ 1 & 0 & 0 \\ 0 & 0 & 0 \end{pmatrix}. \tag{5.15}$$

where $\bar{E}_{ij}^m$ are referred to the $\bar{x}_i$ coordinates. In order to transform $\bar{E}_{ij}^m$ to E_{ij}^m, we use the relation

$$E_{ij}^m = \bar{E}_{kl}^m \gamma_{ik}\gamma_{jl}; \quad \gamma_{ik} = \bar{\boldsymbol{e}}_i \cdot \boldsymbol{e}_k \tag{5.16}$$

where e_i and e_k are the unit vectors parallel to $\bar{x}_i$ and x_k-coordinates. Then for $E_{ij} - E_{ij}^m$, we have

$$E_{ij} - E_{ij}^m = \frac{\kappa}{2}\begin{pmatrix} 0 & 1 & 0 \\ 1 & 0 & 0 \\ 0 & 0 & 0 \end{pmatrix} + \left(\frac{a^2-b^2}{2ab}\right)v\begin{pmatrix} -\sin 2\theta & \cos 2\theta & 0 \\ \cos 2\theta & \sin 2\theta & 0 \\ 0 & 0 & 1 \end{pmatrix}. \tag{5.17}$$

In the present problem, the principal directions are

$$p_i = (\cos\theta, \sin\theta, 0), \quad q_i = (-\sin\theta, \cos\theta, 0), \quad r_i = (0,0,1) \tag{5.18}$$

and we have

$$\frac{C_{ijkl}}{abc}(E_{kl} - E_{kl}^m) = \left(\frac{\kappa}{2}\right)\frac{4\left\{J_1\left(p_ip_j - \frac{1}{3}\delta_{ij}\right) - J_2\left(q_iq_j - \frac{1}{3}\delta_{ij}\right)\right\}}{3(J_1J_2 + J_2J_3 + J_3J_1)}$$

$$+\left(\frac{2}{3I_3}\right)\left(\kappa\cos 2\theta + \frac{a^2-b^2}{ab}v\right)(p_iq_j + p_jq_i) \tag{5.19}$$

5.2.2. The flipping velocity and the tank-treading frequency

Keller and Skalak (1982) analyzed the motion of a tank-treading ellipsoidal cell in a shear flow such as one in Fig. 9. By applying the moment balance on the cell, they found the flipping velocity and they also found the tank-treading frequency by equating the energy dissipated inside the cell and that supplied by the external fluid. By combining the results, they found that the flipping velocity is

$$\dot{\theta} = A + B\cos 2\theta \tag{5.20}$$

where

$$A = -\frac{\kappa}{2}, \quad B = \kappa\left[\frac{4a^2b^2}{a^4-b^4}\left(2 + \left(\frac{\mu'}{\mu} - 1\right)I_3\right)^{-1} + \frac{1}{2}\left(\frac{a^2-b^2}{a^2+b^2}\right)\right],$$

and I_3 is the integral defined as (see Batchelor(1970))

$$I_3 = \int_0^\infty \frac{abc(a^2+b^2)d\lambda}{\Delta(a^2+\lambda)(b^2+\lambda)}$$

with $\Delta^2 = (a^2+\lambda)(b^2+\lambda)(c^2+\lambda)$. As we can see above, the particle undergoes tank-treading motion without flipping if

$0 \le -A/B \le 1$.

The equilibrium angle of inclination is

$$\theta^* = \frac{1}{2}\cos^{-1}\left(-\frac{A}{B}\right) \tag{5.21}$$

and the corresponding tank-treading frequency is

$$v^* = \frac{2ab}{a^2-b^2}\left(\left[2 + \left(\frac{\mu'}{\mu} - 1\right)I_3\right]^{-1}\frac{\kappa A}{B}\right) \le 0 \tag{5.22}$$

On the other hand, if $B < -A$, the cell undergoes the flipping motion. The solution of (5.20) is

$$\theta(t) = \arctan\left\{\frac{A+B}{(A^2-B^2)^{\frac{1}{2}}}\tan\left[\frac{(t-t_0)\pi}{T}\right]\right\} \tag{5.23}$$

where t_0 is the time when $\theta = 0$ and T is the period of flipping from $\theta = 0$ and $\theta = -\pi$. The period T is given by

$$T = \pi(A^2 - B^2)^{-\frac{1}{2}} \tag{5.24}$$

5.2.3. Particle stress for dilute suspension of red blood cells

When the cells undergo tank-treading without flipping, they have of similar shape and orientation. In this case the particle stress is given by

$$\Sigma_{ij}^{(p)} = 3\mu\left(\frac{\Sigma\frac{4}{3}\pi abc}{V}\right)\left(\frac{C_{ijkl}}{abc}\right)(E_{kl} - E_{kl}^{p}) . \tag{5.25}$$

By using the information in (5.19), we can easily show that

$$\frac{\Sigma_{ij}^{(p)}}{3\mu\phi} = \frac{\kappa \sin 2\theta}{3(J_1J_2 + J_2J_3 + J_3J_1)}[J_1X_{ij} - J_2Y_{ij}] + \frac{3\kappa\cos 2\theta}{3I_3}\left[1 - \frac{2}{2 + I_3(\mu'/\mu - 1)}\right]Z_{ij}, \tag{5.26}$$

where

$$X_{ij} = \begin{pmatrix} 1/3 + \cos 2\theta & \sin 2\theta & 0 \\ \sin 2\theta & 1/3 - \cos 2\theta & 0 \\ 0 & 0 & -2/3 \end{pmatrix},$$

$$Y_{ij} = \begin{pmatrix} 1/3 - \cos 2\theta & -\sin 2\theta & 0 \\ -\sin 2\theta & 1/3 + \cos 2\theta & 0 \\ 0 & 0 & -2/3 \end{pmatrix},$$

$$Z_{ij} = \begin{pmatrix} -\sin 2\theta & \cos 2\theta & 0 \\ \cos 2\theta & \sin 2\theta & 0 \\ 0 & 0 & 0 \end{pmatrix},$$

and ϕ is the volume fraction of the red blood cells, i.e. $\phi = \Sigma\frac{4}{3}\pi abc/V$.

When the cells undergo flipping motion, the average particle stress may be obtained as follows.

$$\frac{\overline{\Sigma}_{ij}^{(p)}}{3\mu\phi} = \frac{1}{T}\int_0^T\left(\frac{\Sigma_{ij}^{(p)}}{3\mu\phi}\right)dt = \frac{1}{T}\int_0^{-\pi}\left(\frac{\Sigma_{ij}^{(p)}}{3\mu\phi}\right)\frac{d\theta}{\dot{\theta}} = \frac{1}{T}\int_0^{-\pi}\left(\frac{\Sigma_{ij}^{(p)}}{3\mu\phi}\right)\frac{d\theta}{A + B\cos 2\theta} \tag{5.27}$$

Here we should note that the time average should be the same as that obtained by the probability of distribution. The probability distribution is governed by

$$\frac{\partial p}{\partial t} + \nabla\cdot(p\dot{\theta}\boldsymbol{e}_\theta) = 0 . \tag{5.28}$$

At steady state,

$$\frac{\partial}{\partial\theta}(p\dot{\theta}) = 0 , \ i.e., \ p \propto \frac{1}{\dot{\theta}} \tag{5.29}$$

By using

$$\int_0^{-\pi}\frac{\sin^2 2\theta}{A + B\cos 2\theta}d\theta = \frac{1}{2}\frac{\pi}{(A^2 - B^2)^{\frac{1}{2}}}\left[1 - \frac{B^2/A^2}{\{1 + (1 - B^2/A^2)^{1/2}\}^2}\right] \equiv \frac{T}{2}I_s$$

and

$$\int_0^{-\pi}\frac{\cos^2 2\theta}{A + B\cos 2\theta}d\theta = \frac{1}{2}\frac{\pi}{(A^2 - B^2)^{\frac{1}{2}}}\left[1 + \frac{B^2/A^2}{\{1 + (1 - B^2/A^2)^{1/2}\}^2}\right] \equiv \frac{T}{2}I_c,$$

we may easily show that

$$\frac{\overline{\Sigma}_{ij}^{(p)}}{3\mu\phi} = \left[\frac{(J_1 + J_2)I_s}{3(J_1J_2 + J_2J_3 + J_3J_1)} + \frac{2I_c}{3I_3}\left(1 - \frac{2}{2 + I_3(\mu'/\mu - 1)}\right)\right]E_{ij} \tag{5.30}$$

where

$$E_{ij} = \begin{pmatrix} 0 & \kappa/2 & 0 \\ \kappa/2 & 0 & 0 \\ 0 & 0 & 0 \end{pmatrix}$$

As we can see above, the average particle stress is given in the form of a Newtonian fluid and the effective viscosity is given by

$$\frac{\mu^*}{\mu} = 1 + \left[\frac{(J_1 + J_2)I_s}{2(J_1J_2 + J_2J_3 + J_3J_1)} + \frac{I_c}{I_3}\left(1 - \frac{2}{2 + I_3(\mu'/\mu - 1)}\right)\right]\phi \tag{5.31}$$

The equations (5.26) and (5.31) are the main results of this subsection. For evaluation of the results, we need the shape of tank-treading or flipping red cell. For this purpose, we may need independent theoretical or experimental work.

6. Concluding remarks

For the case of low shear rate limit, we have assumed that the red blood cells form rouleaux that can be considered as long spheroids. By using Bachelor's classic result on the suspension of solid spheroids, a formula for the effective viscosity has been derived in terms of degree of aggregation. In order to find a relationship between the imposed shear rate and the degree of aggregation, we have considered a rouleau in a uniaxial straining flow. By combining two results, a formula for the effective viscosity in terms of the imposed shear rate is obtained. Although very simple and many aspects of rouleau formation are not included in our theoretical model, the theory is capable of showing the shear thinning effect that is in good agreement at least qualitatively with the experimental findings (e.g.

Chien, 1970).

In the limit of high shear rate, the effective viscosity of blood is mainly determined by the deformation characteristics of individual blood cells. For the high shear rate limit, we have considered two problems. One is the problem of completely aligned cells in axisymmetric straining flows and the other is for the case of flipping blood cells in shear flow. Under the axisymetric straining flows, the equilibrium shapes are determined by the sphericity without regard to the given strain rate if the strain rate is high enough for the cells to exist separately. This area preserving constraint has a significant effect on the rheological properties of blood. Indeed, the uniaxial straining viscosity of blood shows quite different characteristics from that of suspension of elastic particles. Elastic particle extends under a straining flow and the surface area of the particle increases as the strain rate increases. Consequently, the effective straining viscosity itself is a strong function of the strain rate. However, in the case of blood cells, the effective viscosity in a straining flow is kept constant for a wide range of strain rate due to the ease of deformation of membrane and the area preserving constraint. From the analysis, it is also found that the effective viscosity of blood is much higher in the uniaxial straining flow than in the biaxial straining flow. This fact must be reflected in the analysis for the flow fields where straining components are predominant. For example, the blood flow in the heart includes straining flow components due to suction and pumping.

Finally, we considered the tank-treading motion of red blood cells. Batchelor's theory on the dilute suspension was modified and it was incorporated with the theory of Keller and Skalak (1982) on the theory of tank-treading motion of red cells. In a shear flow, the red cells may flip or not depending on the shear rate and the cell shape, etc. For the case of tank-treading without flipping, the particle stress is predicted as a function of the shear rate and the aligned angle. In the case of flipping, the low concentration blood shows Newtonian behavior. The predicted formula for the effective viscosity includes an essential parameter which is the shape of the cell. The parameter must be obtained by an independent theoretical or experimental work such as Richardson (1974).

Acknowledgement

This work was supported by the grant from KOSEF through AFERC at POSTECH.

References

Batchelor, G. K., 1970, The stress system in a suspension of forcefree particles, *J. Fluid Mech.* **41**, 545-570.

Chien, S., 1970, *Science* **1970**, 977-979.

Cho, H. J., 1992, M.S. Dissertation, Pohang University of Science and Technology, Korea.

Fung, Y. C., 1981, Biomechanics-Mechanical properties of living tissues, Springer-Verlag, New York.

Goldsmith, H. L., 1971, Red cell motions and wall interaction in tube flow, *Fedn. Proc.* **30**, 1578-1583.

Hinch, E. J. and L. G. Leal, 1972, The effect of Brownian motion on the rheological properties of a suspension of non-spherical particles, *J. Fluid Mech.* **52**, 683-712.

Jeffery, G. B., 1922, The motion of ellipsoidal particles immersed in a viscous fluid, *Proc. R. Soc. Lond.* **A.102**, 161-179.

Kang, I. S., 1992, Annual Report, AFR-92-D, Advanced Fluids Engineering Research Center, Postech, Pohang, Korea.

Keller, S. R. and R. Skalak, 1982, Motion of a tank-treading ellipsoidal particle in a shear flow, *J. Fluid Mech.* **120**, 27-47.

Nakamura, M. and T. Sawada, 1988, Numerical study on the flow of a non-Newtonian fluid through an axisymmetric stenosis, *J. Biomech. Eng.* **110**, 137-143.

Pozrikidis, C. 1990, The axisymmetric deformation of a red blood cell in uniaxial straining Stokes flow, *J. Fluid Mech.* **216**, 231-254.

Richardson, E. 1974, Deformation and haemolysis of red cells in shear flow, *Proc. R. Soc. Lond.* **A.338**, 129-153.

Roscoe, R., 1967, On the rheology of a suspension of viscoelastic spheres in a viscous liquid, *J. Fluid Mech.* **28**, 273-293.

Schmidt-Schönbein, H., R. Wells and J. Goldstone, 1969, Influence of deformability of human red cells on blood viscosity, *Circulation Res.* **25**, 131-143.

Skalak, R., N. Oskaya and T. C. Skalak, 1989, Biofluid Mechanics, *Ann. Rev. Fluid. Mech.* **21**, 167-204.